Plasticity in novel environments induces larger changes in genetic variance than adaptive divergence

Greg M. Walter[1,2*], *Delia Terranova*[3], *James Clark*[1,4], *Salvatore Cozzolino*[5], *Antonia Cristaudo*[3], *Simon J. Hiscock*[4] *and Jon R. Bridle*[1,6]

[1]University of Bristol, School of Biological Sciences, Bristol BS8 1TQ, UK

[2]Current address: Monash University, School of Biological Sciences, Melbourne 3800, Australia

[3]University of Catania, Department of Biological, Geological and Environmental Sciences, Catania 95128, Italy

[4]University of Oxford, Department of Plant Sciences, Oxford, OX1 3RB, UK

[5]University of Naples Federico II, Department of Biology, Naples 80126, Italy

[6]Current address: University College London, Department of Genetics, Evolution and Environment, London WC1E 6BT, UK

* Corresponding Author: Greg M. Walter

Email: greg.walter@monash.edu

Phone: +61 415 246 846

Abstract

Genetic correlations between traits are expected to constrain the rate of adaptation by concentrating genetic variation in certain phenotypic directions, which are unlikely to align with the direction of selection in novel environments. However, if genotypes vary in their response to novel environments, then plasticity could create changes in genetic variation that will determine whether genetic constraints to adaptation arise. We tested this hypothesis by mating two species of closely related, but ecologically distinct, Sicilian daisies (*Senecio*, Asteraceae) using a quantitative genetics breeding design. We planted seeds of both species across an elevational gradient that included the native habitat of each species and two intermediate elevations, and measured eight leaf morphology and physiology traits on established seedlings. We detected large significant changes in genetic variance across elevation and between species. Elevational changes in genetic variance within species were greater than differences between the two species. Furthermore, changes in genetic variation across elevation aligned with phenotypic plasticity. These results suggest that to understand adaptation to novel environments we need to consider how genetic variance changes in response to environmental variation, and the effect of such changes on genetic constraints to adaptation and the evolution of plasticity.

Keywords: adaptive divergence, additive genetic variance, covariance tensor, evolutionary rescue, genotype-by-environment interactions, G-matrix, novel environments, phenotypic plasticity

Introduction

Populations maintain resilience in response to novel environments if selection on existing genetic variation (G) increases fitness over generations to create adaptation (termed 'evolutionary rescue'; Gomulkiewicz and Holt 1995; Bell and Gonzalez 2009), or if the novel environment induces plastic changes for all genotypes (E) that can maintain fitness (Via et al. 1995; Charmantier et al. 2008). In understanding population responses to novel environments, studies often focus on the dichotomy of plasticity versus adaptation for maintaining fitness and avoiding extinction. However, if genotypes vary in their sensitivity to the environment, then genotype-by-environment interactions (G×E) underlying plasticity can change the amount of genetic variation available to selection in novel environments (Wood and Brodie III 2015). Where plasticity can no longer maintain fitness, the potential to persist in a novel environment will then be determined by the extent to which G×E underlying plasticity changes genetic variation, and whether rapid adaptation can ensue (Ghalambor et al. 2007).

The additive genetic variance-covariance matrix (**G**) describes the genetic architecture underlying multivariate phenotypes (Lande 1979). Genetic correlations between traits are expected to concentrate genetic variation in certain directions of the multivariate phenotype. If pleiotropy (or close linkage) underlies genetic correlations, then any genetic changes in one trait will affect other traits similarly and **G** will be stable, which will constrain adaptation when genetic variation lies in directions of the phenotype that differ to selection (Lande 1980; Cheverud 1984; Arnold 1992; Arnold et al. 2008; Walsh and Blows 2009; Chenoweth et al. 2010). However, if **G** changes in response to environmental variation, then G×E can determine the availability of genetic variation in the direction of selection in novel environments, which will then determine whether constraints to adaptation arise (Wood and Brodie III 2015), and therefore the potential for evolutionary rescue.

Although **G** is expected to remain stable, at least in the short term (Zeng 1988), evidence suggests that **G** can change during adaptive divergence (Doroszuk et al. 2008; Eroukhmanoff and Svensson 2011; McGlothlin et al. 2018; Walter et al. 2018) and in response to environmental variation (Wood and Brodie III 2015; Johansson et al. 2020). Evidence also suggests that plasticity in novel environments occurs along phenotypic axes containing large amounts of genetic variation (Noble et al. 2019). However, we do not know whether, or to what extent, shifts in **G** are associated with plasticity in novel environments. If plasticity creates changes in **G**, then such changes in genetic variance can determine the potential for rapid adaptation to maintain ecological resilience in novel environments. Therefore, by quantifying whether changes in **G** occur across environments, and whether such changes align with plasticity, we can better understand how genetic variation present in natural populations can respond to novel environments.

G-matrices can differ in the amount of variance in each trait, as well as in the genetic covariance between traits. **Fig 1a-d** presents an example of how G-matrices for a hypothetical population could change across two environments (A and B). Differences between two matrices can be captured by $\mathbf{C} = \mathbf{G_A} - \mathbf{G_B}$, where **C** is the matrix representing variance that is unique to each G-matrix (**Fig. 1b**). Eigenvectors of **C** then quantify axes that describe the differences in genetic variance between the two original matrices (**Fig. 1c**). Using the eigenvectors of **C** (i.e. the tensor of two matrices), we can test whether differences in **G** align with plastic changes in mean phenotype across environments (**Fig. 1d**). Such an alignment would provide evidence that genotype-by-environment interactions underlying plasticity can change **G**, and determine future evolutionary responses to novel environments.

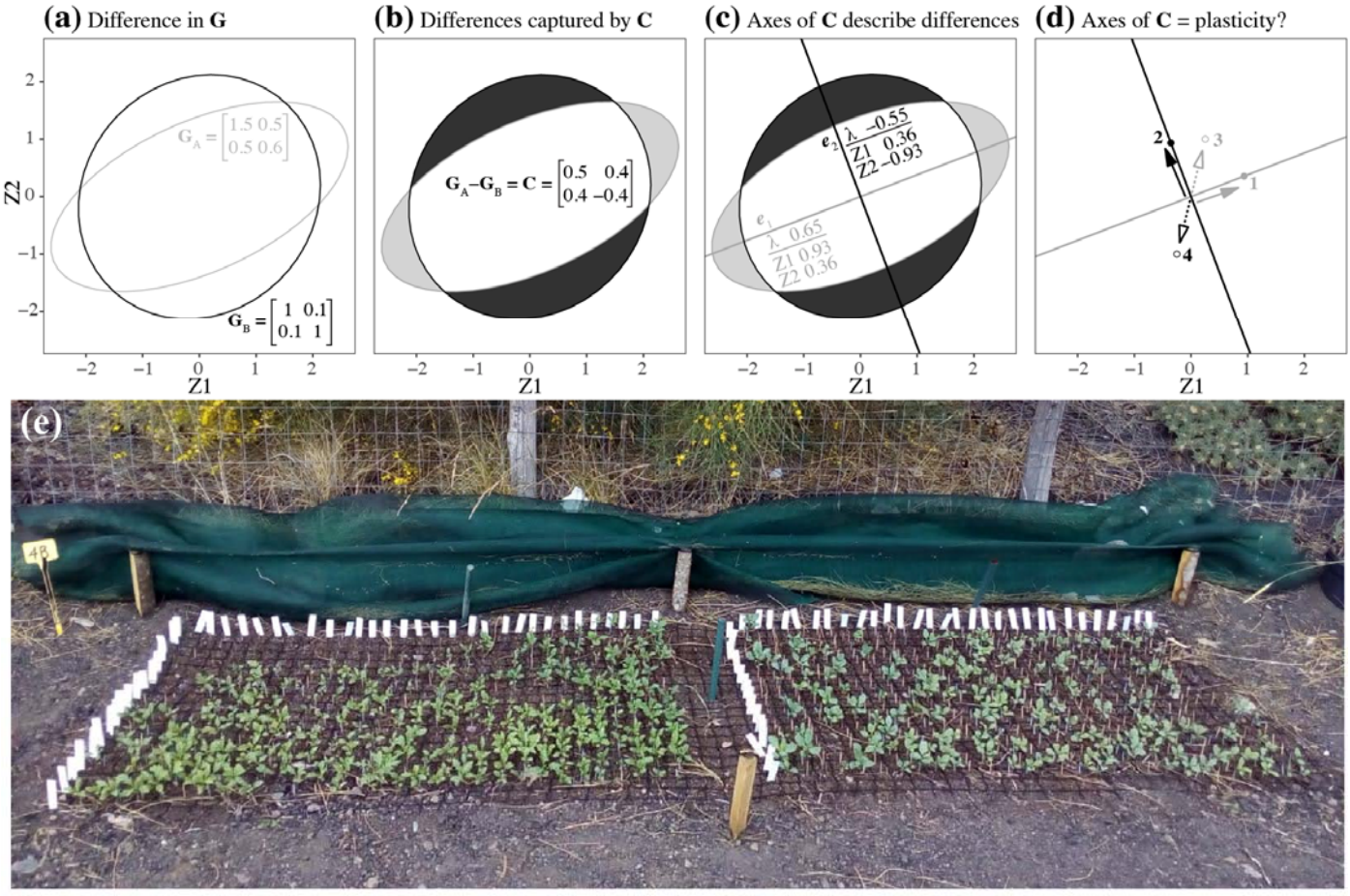

Fig. 1 (a-d) Conceptual diagram demonstrating, for two traits (Z1 and Z2), how differences in **G** for the same population exposed to two environments (A and B) can be quantified with a two-matrix tensor, and then related to plasticity (change in mean phenotype). **(a)** Hypothetical G-matrices are presented in the inset matrices, and visualised as two-dimensional ellipses ($\mathbf{G}_A$ in gray, and $\mathbf{G}_B$ in black). The G-matrices for the two environments (inset tables) differ in shape due to different variances (along the diagonal) and differences in covariances (off-diagonal). **(b)** Differences in **G** are represented by the gray shading for genetic variance unique to environment A, and black shading for genetic variance unique to environment B. These differences in genetic variance can be quantified using $\mathbf{C} = \mathbf{G}_A - \mathbf{G}_B$, which has a positive difference in genetic variance in Z1 (0.5) due to greater

genetic variance in Z1 for environment A. By contrast, Z2 has a negative genetic variance (-0.4) because environment B has greater genetic variance in Z2. **(c)** Decomposing **C** identifies the two major axes (eigenvectors, which in this case are equivalent to eigentensors), which are presented in the inset tables and represented by the black and gray lines. Each eigenvector describes genetic variance that differs between the original matrices (eigenvalues represented by $\boldsymbol{\lambda}$), with the loadings of the traits describing how each trait contributes to the differences in genetic variance described by each eigenvector. The first axis ($\boldsymbol{e}_1$) describes a positive eigenvalue representing differences in genetic variance unique to environment A (gray shading along the gray line). The second axis ($\boldsymbol{e}_2$) describes negative variance describing differences due to genetic variance unique to environment B (black shading along the black line). **(d)** Changes in mean phenotype are represented by arrows and circles. If differences in genetic variance underlie plasticity, we expect changes in mean phenotype along an axis representing genetic variance unique to either environment A (point 1 and solid gray arrow), or environment B (point 2 and black arrow). However, if differences in genetic variance are not associated with plastic responses to the two environments, then changes in mean phenotype would occur along an axis different to changes in genetic variance (points 3 or 4, and dashed lines with unfilled arrows). **(e)** An example of a seedling block at 2,000m, eight weeks after seeds were planted (*S. chrysanthemifolius* on left).

To test whether genotype-by-environment interactions create changes in genetic variance, we reciprocally planted seeds of two ecologically contrasting, but closely related *Senecio* species across an elevational gradient. *Senecio chrysanthemifolius* is a short-lived perennial with dissected leaves that occupies disturbed habitats in the foothills of Mt. Etna (c.400-1,000 m.a.s.l [metres above sea level]), as well as across Sicily. *Senecio aethnensis* is a perennial with entire glaucous leaves endemic to lava flows above 2,000m.a.s.l on Mt. Etna, where individuals grow back each spring after being covered by snow in winter. The data we analyse here are derived from an experiment where we mated among individuals within each species using a quantitative genetics breeding design (Walter et al. 2021). We then reciprocally planted seeds (from each family in the breeding design) of both species across an elevational gradient representing the home range of each species, the edge of their range, and conditions outside their range (**Fig. 1e**). Previously we found evidence for fitness trade-offs as differences in survival at elevational extremes, indicating specialisation of each species to their native environment (Walter et al. 2021).

Here, we continue the analysis of the transplant experiment by including data on leaf morphology and pigment traits, and testing whether genetic variance changes between species and across elevation. Specifically, we test whether: 1) Seedlings show plasticity in novel environments that moves the phenotype towards that of the native species, 2) Elevation or species differences are associated with larger changes in **G**, and 3) Changes in **G** for each species aligned with the direction of plasticity as the elevational change in mean phenotype.

Methods and materials

We only briefly describe the field experiment here, but refer the reader to the previous analysis where it is presented in detail (Walter et al. 2021). We collected cuttings from naturally growing individuals, which we propagated. We randomly assigned each individual as a sire (male) or dam (female) and mated each sire to three dams (*S. aethnensis* *n*=36 sires, *n*=35 dams, *n*=94 full-sibling families; *S. chrysanthemifolius* *n*=38 sires, *n*=38 dams, *n*=108 full-sibling families).

We then planted 100 seeds from each family at four elevations on Mt. Etna that included the native habitats of both species (500m and 2,000m) as well as two intermediate elevations (1,000m and 1,500m). We planted 25 seeds at each site, randomised into five experimental blocks (*S. aethnensis* *n*=432 seeds/block, *n*=2,160 seeds/site; *S. chrysanthemifolius* *n*=540 seeds/block, *n*=2,700 seeds/site; Total N=19,232 seeds). To prepare each experimental block, we cleared the ground of plant matter and debris, and then placed a plastic grid on the ground with 4cm square cells. We attached each seed to the middle of a toothpick using non-drip super glue and then pushed each toothpick into the soil so that the seed sat 1-2mm below the soil surface. To replicate natural germination conditions, we suspended 90% shade-cloth 20cm above each plot and kept the seeds moist until germination ceased (2-3 weeks). After this shade-cloth was removed and watering reduced.

When >80% of plants had produced ten leaves at each transplant site, we collected the 5th and 6th leaves from the base of the plant to quantify morphology and leaf pigment content. In total, we measured 6,454 plants (500m *n*=2,369; 1,000m *n*=1,929; 1,500m *n*=1,030; 2,000m *n*=1,126), which included more than two individuals for >90% of the full-sibling families at each elevation (average number of individuals measured per family: 500m=11.73±5.5[one standard deviation], 1,000m=9.55±3.7, 1,500m=5.10±2.8, 2,000m=5.57±3.1). This meant that all sires were measured at each site, and that mortality should not influence the estimation of genetic variance. To quantify leaf pigment content, we used a Dualex instrument (Force-A, France) to estimate the chlorophyll, flavonol and anthocyanin content of each leaf. To measure leaf morphology, we scanned the leaves (Canoscan 9000F) and quantified morphology using the software Lamina (Bylesjo et al. 2008), which produced leaf morphology traits that included leaf area, leaf complexity ($\frac{\text{leaf perimeter}^2}{\text{leaf area}}$), the width of leaf indents, and the number of leaf indents standardised by perimeter. We then weighed the leaves of each plant and calculated specific leaf area (SLA = $\frac{leaf\ area}{leaf\ weight}$). To analyse phenotype data, we used R (v.3.6.1; R Core Team 2019) for all analyses. Prior to analysis, we standardised each trait by their mean so that traits measured on different scales could be compared (Hansen and Houle 2008).

1. Species differences in plasticity across elevation

To quantify species differences in phenotypic plasticity across the elevational gradient, we used a

Multivariate Analysis of Variance (MANOVA), which tested for significant differences in mean multivariate phenotype across elevation. We included all eight phenotypic traits as the multivariate response variable. Elevation, species and their interaction were included as fixed effects. To visualise how the two species differed across elevation we first constructed a D-matrix, the covariance matrix representing differences in mean multivariate phenotype between species and across elevation (see glossary in **Table 1**). To construct **D**, we extracted the Sums of Squares and Cross-Product (SSCP) matrices for each fixed effect ($SSCP_S$ = species; $SSCP_E$ = elevation; $SSCP_{S\times E}$ = species×elevation) and the error term ($SSCP_R$). We then estimated $SSCP_H$ ($SSCP_H = SSCP_S + SSCP_E + SSCP_{S\times E}$), which calculates the difference in mean across all elevations for both species. We calculated Mean Square (MS) matrices by dividing the SSCP matrices by their corresponding degrees of freedom ($MS_H = \frac{SSCP_H}{7}$; $MS_E = \frac{SSCP_E}{6,446}$). We then estimated **D** using

$$\mathbf{D} = \frac{MS_H - MS_E}{nf}, \qquad (1)$$

where *nf* represents the average number of individuals measured for each species at each elevation, calculated from equation 9 in Martin et al. (2008). We used the eigenvectors of **D** to visualise differences in multivariate phenotype across elevation for both species.

2. Quantifying species and elevational differences in genetic variance

Estimation of additive genetic variance: The additive genetic (co)variance matrix (**G**) represents the multivariate genetic variance underlying morphological traits. To calculate **G** for each species at each elevation, we used the package *MCMCglmm* (Hadfield 2010) and implemented the multivariate linear mixed model

$$y_{ijkl} = s_{i(j)} + d_{j(i)} + b_k + e_{l(ijk)}, \qquad (2)$$

where $s_{i(j)}$ represents the *i*th sire mated to the *j*th dam, $d_{j(i)}$ the *j*th dam mated to the *i*th sire, b_k as the variance among blocks within a transplant site and $e_{l(ijk)}$ the residual error. The eight normally distributed phenotypic traits were included as the multivariate response variable (y_{ijkl}). We applied equation 2 separately to each species and transplant elevation, resulting in the estimation of eight G-matrices. For each implementation, we extracted the sire variance component and multiplied it by four to calculate our observed G-matrices (Lynch and Walsh 1998).

We implemented equation 2 using chains with a burn-in of 300,000 iterations, a thinning interval of 1,500 iterations and saving 2,000 iterations that provided the posterior distribution for all parameters estimated. We confirmed model convergence by checking that the chains mixed sufficiently well and that autocorrelation

was lower than 0.05, and that our parameter-expanded prior was uninformative.

To test whether our experimental design captured biologically meaningful estimates of genetic variance, for each implementation of equation 2, we randomised offspring among sires and dams, and re-applied the model to the randomised data. To maintain differences among the experimental blocks, we randomised the parentage of offspring within each block separately. We conducted 1,000 randomisations for each observed G-matrix, which we used to estimate our randomised G-matrices representing the null distribution for our estimation of **G**. Observed estimates of genetic variance that exceed the null distribution provides strong evidence that our estimates of genetic variance are statistically significant.

Table 1 Glossary of quantitative genetics terms

Term	Sym-bol	Definition
D-matrix	**D**	The variance-covariance matrix of mean phenotype. This captures how a group of traits differs in multivariate mean among levels of a covariate (e.g., elevation)
G-matrix	**G**	The additive genetic variance-covariance matrix underlying a set of traits. Genetic variances on the diagonal and genetic covariances among traits off the diagonal
$\boldsymbol{d}_{max}$		The first eigenvector of **D**, representing the axis along which the greatest differences in mean multivariate phenotype lie
$\boldsymbol{g}_{max}$		The first eigenvector of **G**, representing the axis that describes the direction containing the greatest amount of additive genetic variance
Sire variance		If a group of randomly selected sires are each mated to multiple dams in a breeding design, the variance among the sires represents 1/4 of the additive genetic variance after accounting for variance among dams and full-siblings
S-matrix	**S**	A symmetric matrix used for a tensor analysis. **S** describes the element-by-element differences among the original matrices
Eigentensor	**E**	Orthogonal axes describing differences among the original matrices. Eigentensors are constructed by scaling and arranging eigenvectors of **S**
Eigenvector (*n*) of eigentensor (*p*)	$\boldsymbol{e}_{p,n}$	The set of *n* eigenvectors that describe the *p*th eigentensor. Trait loadings describe how each trait contributes to differences among the original matrices that are captured by the eigenvector of an eigentensor.
Coordinates of an eigentensor		The correlation between the original matrices and each eigentensor. Quantifies which matrices contribute to the differences among all matrices that are captured by an eigentensor.

186

187 *Quantifying differences in genetic variance:* To quantify differences in **G**, we used a covariance tensor
188 approach (see glossary in **Table 1**). The strength of this approach is that, unlike other methods that focus on
189 pairwise comparisons, the covariance tensor can simultaneously compare multiple matrices. This simply
190 extends the two-matrix example (presented in **Fig. 1a-c**) to three or more matrices. The covariance tensor
191 quantifies differences among multiple matrices by first quantifying a matrix (the S-matrix) that captures the
192 raw differences among all matrices, and then identifying how each of the original traits and matrices
193 contribute to the differences captured by **S**. We only briefly describe the approach here, and refer readers to
194 more detailed descriptions in Basser and Pajevic (2007); Hine et al. (2009); Aguirre et al. (2014); Walter et
195 al. (2018), and a simplified description (**Fig. S4**). The covariance tensor is based on decomposition (i.e.
196 eigenanalysis, which is analogous to principal components) of symmetric matrices to construct a set of
197 orthogonal axes, known as eigentensors, which are used to identify and describe differences in the original
198 matrices being compared (e.g., elevation).

199 First, a symmetric matrix (**S**) is calculated, whose elements represent element-by-element variation among
200 the original matrices. Decomposing **S** identifies the orthogonal axes (eigenvectors) along which the original
201 matrices differ the most. Eigenvectors are scaled and rearranged to calculate the eigentensors, which are used
202 to identify how the original traits and matrices contributed to differences among all matrices. To identify
203 whether the observed eigentensors described significant differences in genetic variance, we constructed a null
204 distribution by randomising sire breeding values among treatments (here, elevations), and calculating a
205 randomised G-matrix for each MCMC iteration from the observed models. This calculates a null-distribution
206 based on the structure of the observed G-matrices (Aguirre et al. 2014). However, as suggested by Morrissey
207 et al. (2019), we also tested for significant eigentensors by randomising the sires among species and
208 elevations in the original dataset and re-implementing equation 2 on each randomisation. If the observed
209 eigentensors described greater differences in genetic variance than the eigentensors constructed from the null
210 distribution, then there is strong evidence for significant differences in our observed **G**.

211 To identify how each matrix (in our case, one elevation for a given species) contributes to differences among
212 all matrices (all elevations for a given species), the matrix coordinates of the eigentensors are calculated. The
213 coordinates are linear combination scores that are calculated between each eigentensor and the original
214 matrices, and can be interpreted similarly to a principal components analysis: larger scores indicate a greater
215 correlation between any given matrix and the differences among matrices described by that particular
216 eigentensor.

To identify how the original traits contribute to differences among matrices, each eigentensor is decomposed, and the eigenvectors interpreted in the same fashion as a principal components analysis. Traits with large loadings contribute to the differences described by the eigenvector of a particular eigentensor. Traits with loadings of different signs (positive and negative) describe traits that contribute to the differences in opposite ways. To identify how strongly each of the original matrices are associated with each eigenvector, we can use the matrix projection

$$\mathrm{V}_{ijk} = \boldsymbol{e}_{ij}^{T}\mathbf{G}_{k}\boldsymbol{e}_{ij}\,, \qquad (3)$$

where the V_{ijk} quantifies the amount of variance in the G-matrix from the *k*th elevation that is described by the *j*th eigenvector from the *i*th eigentensor ($\boldsymbol{e}_{i,j}$). Greater values of V_{ijk} for any given matrix suggest that differences in that particular matrix underlie the differences in genetic variance captured by that eigenvector of the eigentensor.

We used the covariance tensor approach to make two comparisons. First, to identify whether elevation or adaptive divergence (i.e. differences between species) created larger differences in **G**, we compared the G-matrices of the two elevational extremes for both species. If adaptive divergence (i.e. exposure to different environments during the process of ecological speciation) created greater changes in **G** than exposure to current environmental variation (i.e. to the elevational gradient), then differences between species would be greater than differences across elevation. Second, to identify the extent of elevational changes in **G**, we quantified changes in **G** across elevation for each species separately.

3. Testing whether elevational changes in genetic variance are associated with plasticity

To test whether elevational changes in G were associated with plasticity (change in mean phenotype), we compared the eigenvectors of eigentensors (capturing differences in **G**) with a D-matrix representing multivariate change in phenotype across elevation. First, we conducted MANOVA as before, but for each species separately, and including experimental block (within elevation) as the error term, which tests whether elevational differences in mean multivariate phenotype are significantly greater than differences among blocks within elevation. We then used the output of the MANOVA to calculate a D-matrix that captured the elevational change in mean phenotype for each species. Second, we used matrix projection (equation 3), to project the eigenvectors of eigentensors through the D-matrix for each species separately. We predicted that if G×E underlying plasticity can change the structure of **G**, then eigenvectors (of eigentensors) that describe the largest differences in **G** would also describe large changes in mean multivariate phenotype.

Estimating G×E across elevation: We tested whether plasticity was associated with G×E as a change in variance or as changes in rank of sire breeding values across elevation. We calculated the scores for the

first two eigenvectors of **D** (from equation 1) and used equation 2 to estimate the genetic variance at each elevation, and the genetic covariance among elevations. For each random component, we specified random slopes and intercepts for elevation. To specific the correct residual variance structure, we only estimated the residual variances at each elevation because two plants were not present at more than one elevation, preventing the estimation of residual covariance among elevations.

Results

1. Species differed in their change in mean phenotype across elevation

The MANOVA provided evidence that species (Wilks' $\lambda = 0.21$, $F_{1,6446} = 2940.56$, $P<0.0001$), elevation (Wilks' $\lambda = 0.30$, $F_{3,6446} = 401.12$, $P<0.0001$) and their interaction (Wilks' $\lambda = 0.83$, $F_{3,6446} = 50.62$, $P<0.0001$) all showed significant differences in mean multivariate phenotype. Changes in the univariate trait means are presented in **Fig. S2**. We used the MANOVA to estimate a D-matrix representing differences in mean multivariate phenotype between species and across elevation. We found that *S. chrysanthemifolius* shows a relatively gradual change in phenotype across elevation (**Fig. 2**). By contrast, *S. aethnensis* shows a sharper change in mean phenotype whereby the highest elevation (i.e., the native elevation) contrasts with all three lower elevations (**Fig. 2**).

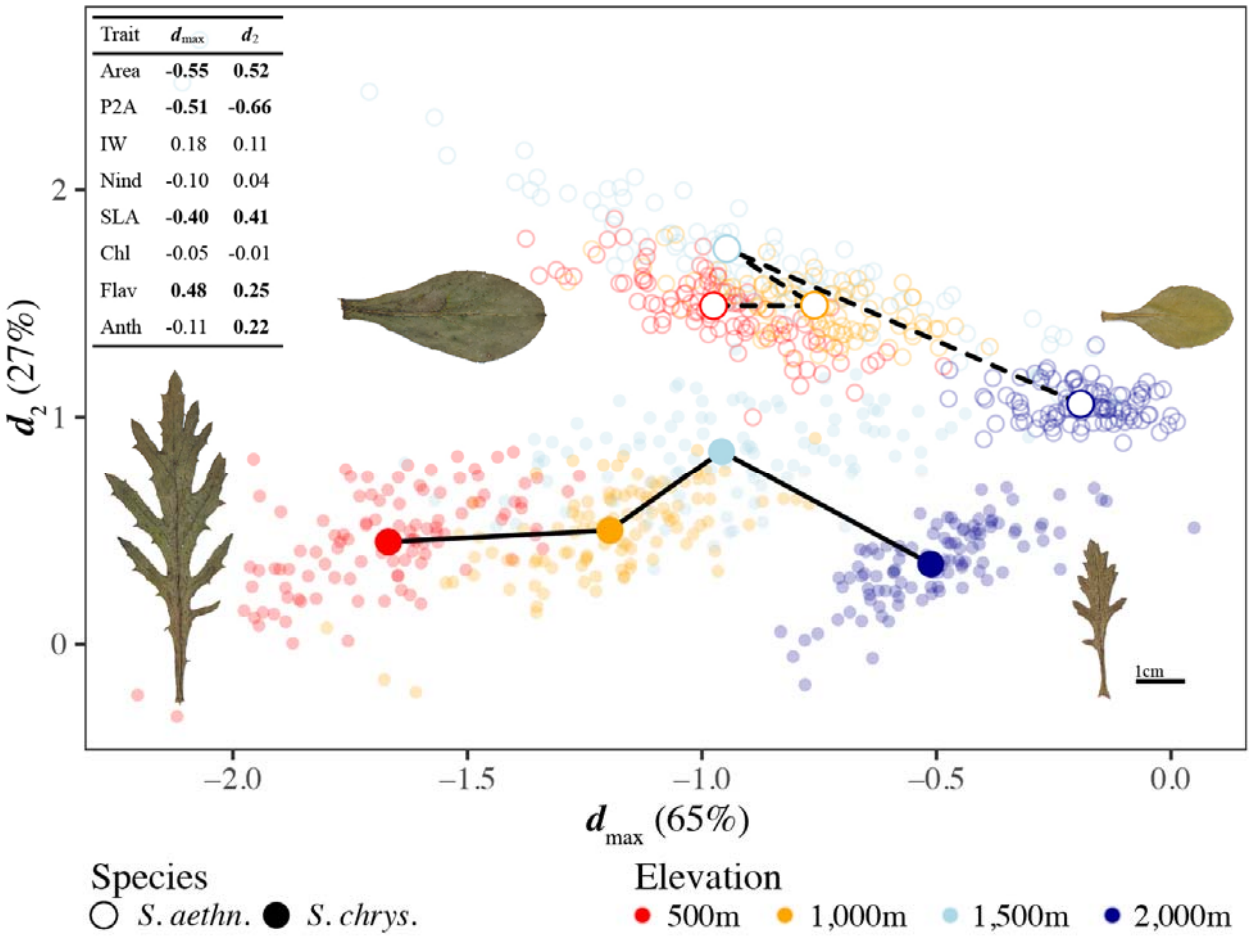

Fig. 2 Phenotypic plasticity creates large changes in mean multivariate phenotype. The first two axes of **D** together represent 92% of all change in mean phenotype, with the table inset displaying the trait loadings for each axis (loadings in bold contribute substantially to each axis). Large coloured circles represent the mean of each species at each transplant site, with the size of the circle exceeding one standard error. Small circles represent the mean for each full-sibling family. Inset leaves represent a plant near the mean phenotype of each species for the elevational extremes.

2. Genetic variance changed more across elevation than between species

We quantified G-matrices for each species and at each elevation (**Table S2**), and decomposed each matrix to identify the orthogonal axes (known as eigenvectors) that describe the distribution of genetic variance within each G-matrix (**Table 2**). The first four eigenvectors of **G** together described more than 80% of all genetic variance (**Table 2**), and were greater than expected under random sampling (**Fig. S2**), which suggests that our matrices captured biologically meaningful genetic variance underlying morphology. G-matrices can differ in size (the total amount of genetic variance), shape or orientation. If all traits are genetically independent, all axes of a G-matrix will describe a similar amount of genetic variance, and the matrix will be spherical. However, the shape of a G-matrix becomes more elliptical when genetic correlations among traits condense genetic variance into fewer axes (than the number of traits) that contain higher proportions of the

total genetic variance. Differences in shape arise when matrices are more or less elliptical. Differences in orientation arise when the linear combination of traits that are used to describe the major axes of genetic variance differ between matrices.

Compared to the G-matrices estimated at the three lower elevations (500m-1,500m), we found that the G-matrices of both species were smaller (i.e., contained less genetic variance) at the highest elevation (**Table 2** and **Table S2**). *Senecio aethnensis* showed a similar shape across elevation, whereby three axes consistently described >80% of the genetic variance at each elevation (**Table 2**). By contrast, G-matrices of *S. chrysanthemifolius* were more elliptical at lower elevations (two axes described >70% of total genetic variance), and much more spherical at the highest elevation (four axes described 80% of total genetic variance). For both species the magnitude and sign (positive vs negative) of trait loadings changed across elevation (**Table 2**), suggesting that different linear combinations of traits described axes of **G** at different elevations.

Table 2 The first four eigenvectors describing >80% of total genetic variation for each G-matrix estimated at each elevation for: **(a)** *S. aethnensis*, and **(b)** *S. chrysanthemifolius*. HPD represents the upper and lower 95% Highest Posterior Density intervals. 'Proportion' quantifies the proportion of total genetic variance that each eigenvector describes, and 'Cumulative' represents the cumulative proportion of genetic variance. Trait loadings in bold are greater than 0.2 to aid interpretation of the eigenvectors.

	500m				**1,000m**				**1,500m**				**2,000m**			
	$\boldsymbol{g}_{max}$	$\boldsymbol{g}_2$	$\boldsymbol{g}_3$	$\boldsymbol{g}_4$	$\boldsymbol{g}_{max}$	$\boldsymbol{g}_2$	$\boldsymbol{g}_3$	$\boldsymbol{g}_4$	$\boldsymbol{g}_{max}$	$\boldsymbol{g}_2$	$\boldsymbol{g}_3$	$\boldsymbol{g}_4$	$\boldsymbol{g}_{max}$	$\boldsymbol{g}_2$	$\boldsymbol{g}_3$	$\boldsymbol{g}_4$
(a) *S. aethnensis*																
Eigenvalues	0.046	0.031	0.020	0.007	0.049	0.020	0.011	0.008	0.050	0.026	0.014	0.008	0.019	0.014	0.009	0.007
HPDlwr	0.020	0.011	0.008	0.001	0.022	0.008	0.003	0.001	0.019	0.002	0.005	0.001	0.002	0.004	0.003	0.001
HPDupp	0.076	0.053	0.034	0.017	0.080	0.034	0.022	0.018	0.084	0.064	0.025	0.021	0.038	0.026	0.017	0.020
Proportion	0.41	0.27	0.18	0.06	0.51	0.20	0.12	0.08	0.45	0.23	0.12	0.07	0.30	0.22	0.15	0.12
Cumulative	0.41	0.68	0.86	0.92	0.51	0.71	0.83	0.91	0.45	0.68	0.80	0.87	0.30	0.52	0.67	0.79
Traits:																
Area	0.19	**0.33**	0.04	-0.12	0.17	**0.45**	**0.67**	**-0.54**	**0.20**	**0.86**	**-0.44**	0.16	**0.21**	**0.29**	**0.26**	**0.87**
P2A	0.12	**-0.41**	**0.88**	0.07	**0.30**	**-0.83**	**0.44**	-0.08	**0.34**	**-0.52**	**-0.70**	**0.32**	**-0.47**	**-0.71**	**0.22**	**0.30**
Nind	**-0.51**	**-0.39**	-0.04	**-0.33**	**-0.26**	**-0.22**	**-0.29**	**-0.58**	**-0.59**	0.02	**-0.25**	-0.05	**-0.30**	0.01	-0.06	-0.10
IW	**0.47**	**0.28**	0.17	**0.27**	**0.24**	0.18	**0.25**	**0.55**	**0.64**	0.03	**0.33**	-0.01	0.17	-0.08	0.01	0.13
SLA	0.04	**-0.23**	**-0.23**	**0.63**	0.17	0.15	-0.16	**-0.20**	-0.03	-0.03	-0.16	**-0.53**	-0.07	**0.20**	**-0.76**	**0.20**
Chl	0.00	**0.34**	**0.20**	**-0.33**	-0.13	-0.08	0.06	0.11	0.10	0.00	**0.24**	0.13	**0.48**	-0.13	0.16	-0.14
Flav	**-0.69**	**0.50**	**0.29**	**0.43**	**-0.83**	-0.04	**0.42**	0.13	**-0.26**	0.02	**0.24**	**0.75**	0.08	**0.27**	**0.46**	**-0.27**
Anth	-0.03	**-0.27**	-0.08	**0.34**	0.15	0.06	0.06	-0.07	-0.05	-0.01	-0.04	0.06	**-0.61**	**0.53**	**0.23**	-0.01
(b) *S. chrysanthemifolius*																
Eigenvalues	0.053	0.027	0.016	0.012	0.048	0.023	0.010	0.004	0.022	0.015	0.013	0.010	0.028	0.009	0.005	0.004
HPDlwr	0.024	0.012	0.007	0.004	0.020	0.011	0.001	0.001	0.005	0.001	0.002	0.001	0.003	0.000	0.000	0.000
HPDupp	0.087	0.044	0.028	0.022	0.083	0.039	0.023	0.008	0.041	0.035	0.028	0.025	0.058	0.022	0.013	0.013
Proportion	0.45	0.23	0.14	0.11	0.52	0.25	0.10	0.04	0.29	0.20	0.17	0.14	0.52	0.16	0.09	0.08
Cumulative	0.45	0.68	0.82	0.93	0.52	0.77	0.87	0.91	0.29	0.49	0.66	0.80	0.52	0.68	0.77	0.85
Traits:																
Area	**-0.21**	**0.74**	**-0.22**	**0.57**	**0.25**	-0.07	**0.92**	**0.21**	**0.43**	**0.53**	-0.05	**0.67**	-0.03	**-0.52**	**0.74**	**-0.38**
P2A	**-0.91**	**-0.35**	0.07	0.16	**-0.92**	0.02	**0.31**	**-0.23**	**-0.47**	**0.64**	**-0.52**	**-0.20**	**-0.97**	0.07	0.00	-0.05
Nind	0.10	**-0.30**	**-0.45**	0.11	0.02	**0.65**	0.04	**0.22**	**0.55**	0.11	0.01	**-0.38**	0.18	**0.58**	**0.38**	-0.03
IW	-0.05	**0.32**	**0.65**	-0.18	0.07	**-0.68**	-0.02	-0.07	**-0.41**	**-0.30**	-0.03	**0.35**	0.05	**-0.53**	**-0.34**	0.09
SLA	0.03	0.11	**-0.46**	-0.07	0.03	-0.01	-0.02	0.01	0.04	**0.20**	0.08	-0.15	-0.01	0.13	**0.23**	-0.03
Chl	0.01	0.07	0.01	-0.16	0.08	0.13	0.08	0.11	**0.32**	**-0.32**	**-0.73**	-0.17	0.09	-0.12	-0.17	**-0.27**
Flav	**0.34**	**-0.35**	**0.32**	**0.73**	**0.29**	**0.23**	0.14	**-0.91**	0.13	0.04	0.14	0.06	0.10	**-0.22**	0.07	0.09
Anth	-0.01	0.02	0.11	0.18	0.04	**-0.21**	0.15	-0.13	-0.07	**0.24**	**0.41**	**-0.43**	-0.05	-0.16	**0.32**	**0.87**

The first axis of **G**, $\boldsymbol{g}_{max}$, describes the greatest amount of genetic variance. It is expected that $\boldsymbol{g}_{max}$ will remain stable due to pleiotropy preventing independent changes in different traits. However, for *S. aethnensis* we found that all elevations were nearly orthogonal to the home site (angle between $\boldsymbol{g}_{max}$ at the home site

[2,000m] and $\boldsymbol{g}_{max}$ at: 1,500m=76.2°; 1,000m=77.8°; 500m=79.7°). By comparison, for *S. chrysanthemifolius* the angle between the home site (500m) and the other elevations were much lower (1,000m=28.3°; 1,500m=62.2°; 2,000m=20.1°).

***G** changes more across elevation than between species:* To quantify differences in **G** we used a covariance tensor approach, which we applied to two separate analyses. To test whether species or elevation created larger changes in **G**, we applied a covariance tensor to the G-matrices of both species at the elevational extremes (both native elevations). Elevational differences in **G** appear to be substantial for both species (**Fig. 3a**, **Table2** and **Fig. S5**). Using the covariance tensor to quantify differences in genetic variance, we found that two (of three) eigentensors described greater differences in genetic variance compared to the null expectation (**Fig. S3a**). The coordinates capture how each matrix contributes to the differences described by an eigentensor. The first eigentensor, which captures 31.9% of all differences among G-matrices, describes large differences between extreme elevations, but not between species (**Fig. 3b**). By contrast, the second eigentensor captures 26.2% of all differences among G-matrices, and describes large differences between species, but not between elevations (**Fig. 3b**). Therefore, elevation created larger changes in **G** than adaptive divergence between the two species.

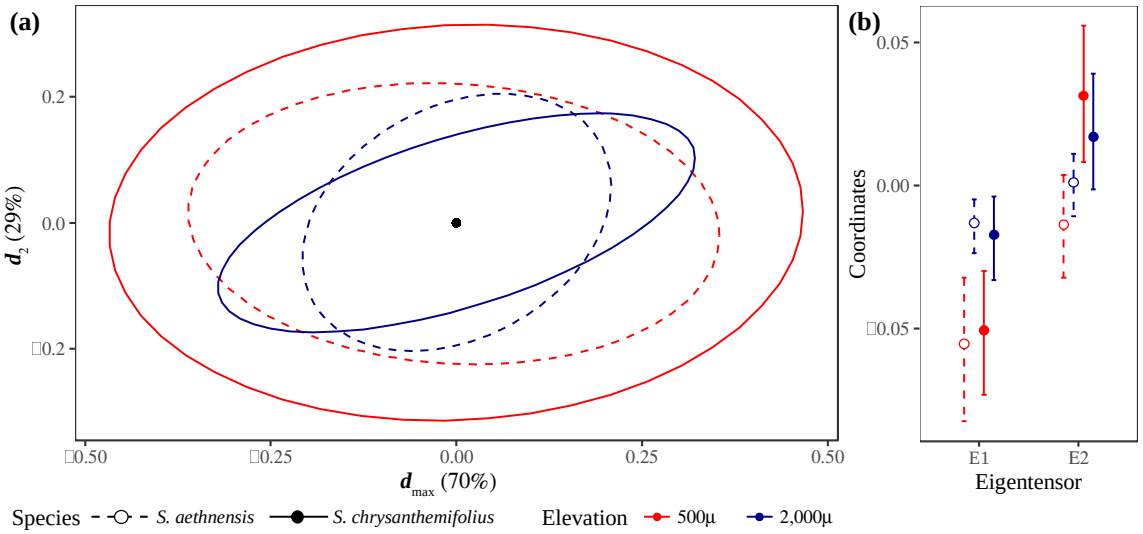

Fig. 3 Differences in **G** are greater across elevational extremes than between species. **(a)** Visualising differences between species at the elevational extremes shows that the two species differ in their G-matrices, and that they respond to elevation differently. **(b)** The coordinates quantify how each matrix contributes to differences in genetic variance described by each eigentensor. Credible intervals represent the 95% HPD (Highest Posterior Density) intervals. The first eigentensor (describing 31.9% of the total difference in genetic variance) describes differences between the elevational extremes, but not differences between species. By contrast, the second eigentensor (describing 26.2% of the total difference in genetic variance) describes differences between species, but not between elevations. The summary of the tensor is located in **Table S3a**.

Second, we used the covariance tensor approach to quantify changes in **G** across elevation for each species separately. Visualising the G-matrices of the two species suggests large changes across elevation (**Fig. 4a**). We found that two eigentensors for *S. aethnensis*, and one eigentensor for *S. chrysanthemifolius* capture greater differences in genetic variance than expected under random sampling (**Fig. S3b-c**). For *S. aethnensis*, the coordinates of the first eigentensor reveal strong differences in **G** between 2,000m and the lower elevations, while the second eigentensor quantifies differences between the two upper and lower elevations (**Fig. 4b**). Similarly, the first eigentensor captures differences between the upper and lower elevations for *S. chrysanthemifolius* (**Fig. 4b**). Projecting the eigenvectors of eigentensors through the original G-matrices reveals how each original matrix (i.e. each elevation) contributes to the differences in genetic variance described by that particular eigenvector. We present only the first four eigenvectors from each eigentensor because these describe >80% of the differences captured by each eigentensor. Eigenvectors of eigentensors describe significant differences in genetic variance across elevation (**Fig. 4c**).

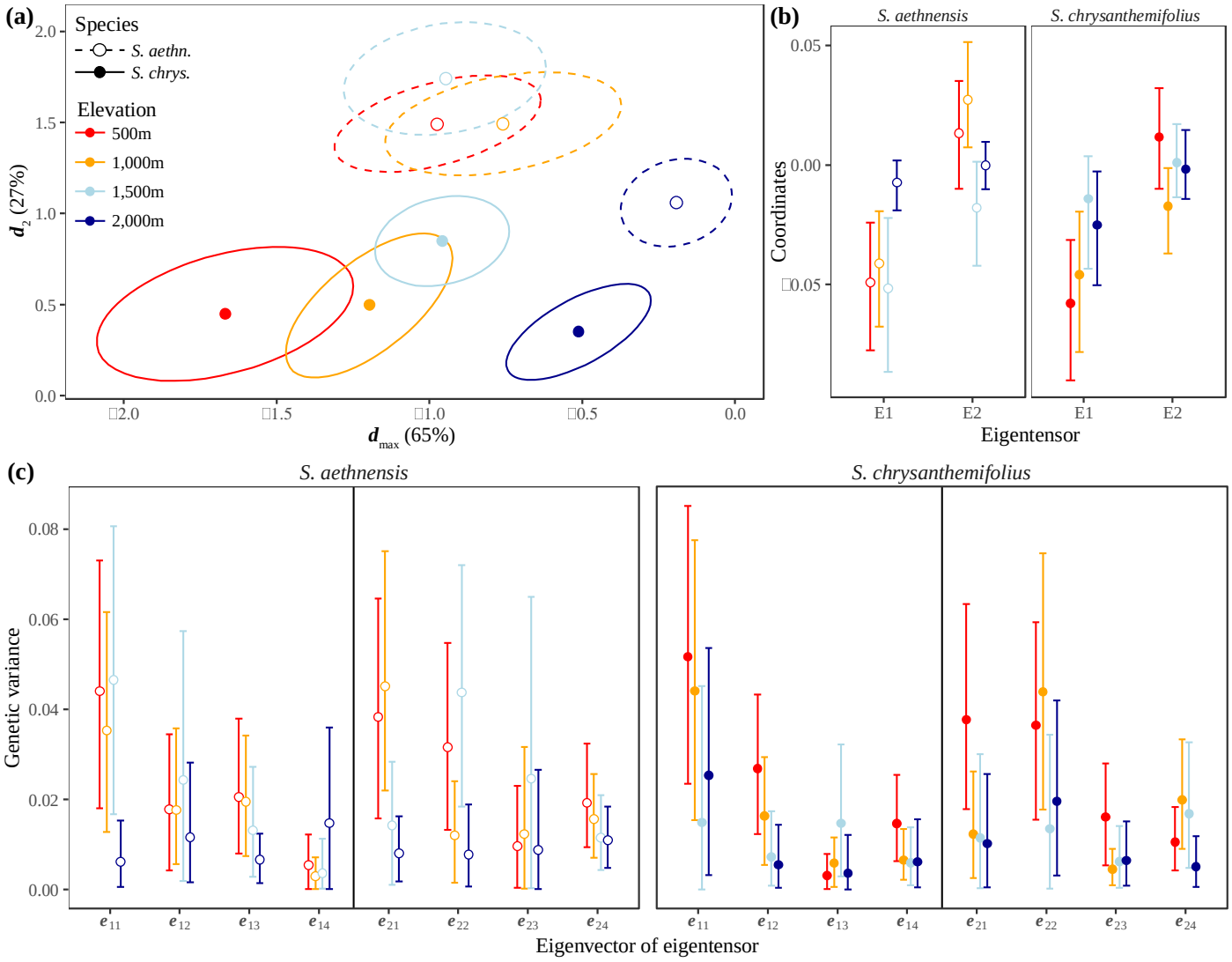

Fig. 4 Elevation induces changes in **G** for both species. **(a)** Visualising G-matrices for both species at all elevations shows how

they change with the change in mean phenotype. **(b)** The coordinates show that, for both species, the first two eigentensors describe elevational differences in genetic variance. Credible intervals represent the 95% HPD intervals. **(c)** To identify how each elevation contributes to differences in **G** captured by the eigenvectors of eigentensors, we use matrix projection. G-matrices that describe more variance for a given eigenvector (of an eigentensor) contribute to the differences in elevation described by that particular eigenvector of the eigentensor. We only present the first four eigenvectors because they describe >80% of the difference in genetic variance captured by each eigentensor. The tensor summaries are located in **Table S3b-c**.

3. Changes in genetic variance are associated with changes in mean phenotype

If G×E interactions that change **G** are associated with plasticity, we predicted that elevational differences in **G** would align with plastic changes in mean phenotype. To test this (for each species separately), we projected the eigenvectors of eigentensors (from **Fig. 4c**), which capture the greatest differences in **G**, through the D-matrix (representing elevational differences in mean multivariate phenotype). If changes in **G** were associated with plasticity, then eigenvectors of eigentensors that describe the greatest differences in **G** (i.e. the leading eigenvectors of each eigentensor) would also describe more variance in **D** than expected under random sampling. We found that for both species, our results supported our predictions, and that this was particularly strong for *S. chrysanthemifolius* (**Fig. 5**).

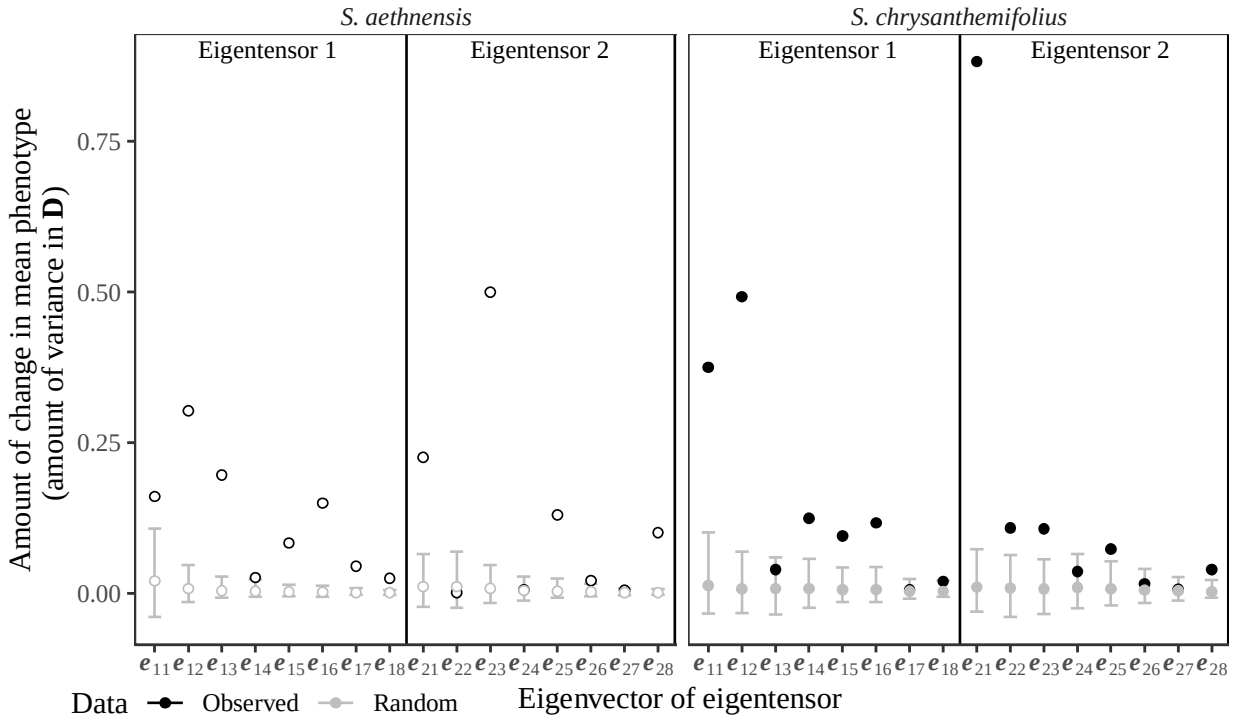

Fig. 5 Eigenvectors of eigentensors that describe large differences in **G** also describe large changes in mean multivariate phenotype. The first two eigenvectors of each eigentensor capture >90% of the difference in genetic variance described by that eigentensor. We predicted that if the first two eigenvectors (that capture the greatest difference in genetic variance) describe large differences in mean multivariate phenotype, then changes in **G** align with plasticity. Projecting the eigenvectors of eigentensors

through the observed D-matrix (black circles) shows that the leading eigenvectors from each eigentensor describe greater differences in mean phenotype than expected under random sampling (gray circles and credible intervals representing 95% HPD intervals) and describe the greatest difference in mean phenotype. Therefore, we found evidence that changes in **G** align with plastic changes in mean phenotype.

Changes in **G** *are associated with G×E in plasticity:* Estimating the G-matrix for the axis representing the largest change in mean phenotype ($\boldsymbol{d}_{max}$), quantifies the genetic variance at each elevation and the genetic covariance between elevations. We found evidence of G×E as large changes in genetic variance across elevation, with much smaller amounts of genetic variance at high elevation for both species (**Fig. 6**; **Table S4**). Genetic correlations between elevations are moderately strong and range from 0.42 to 0.72 (**Table S4**). Genetic correlations between elevations of less than one suggest that G×E is also present as a change in sire rank across elevation (**Fig. 6**).

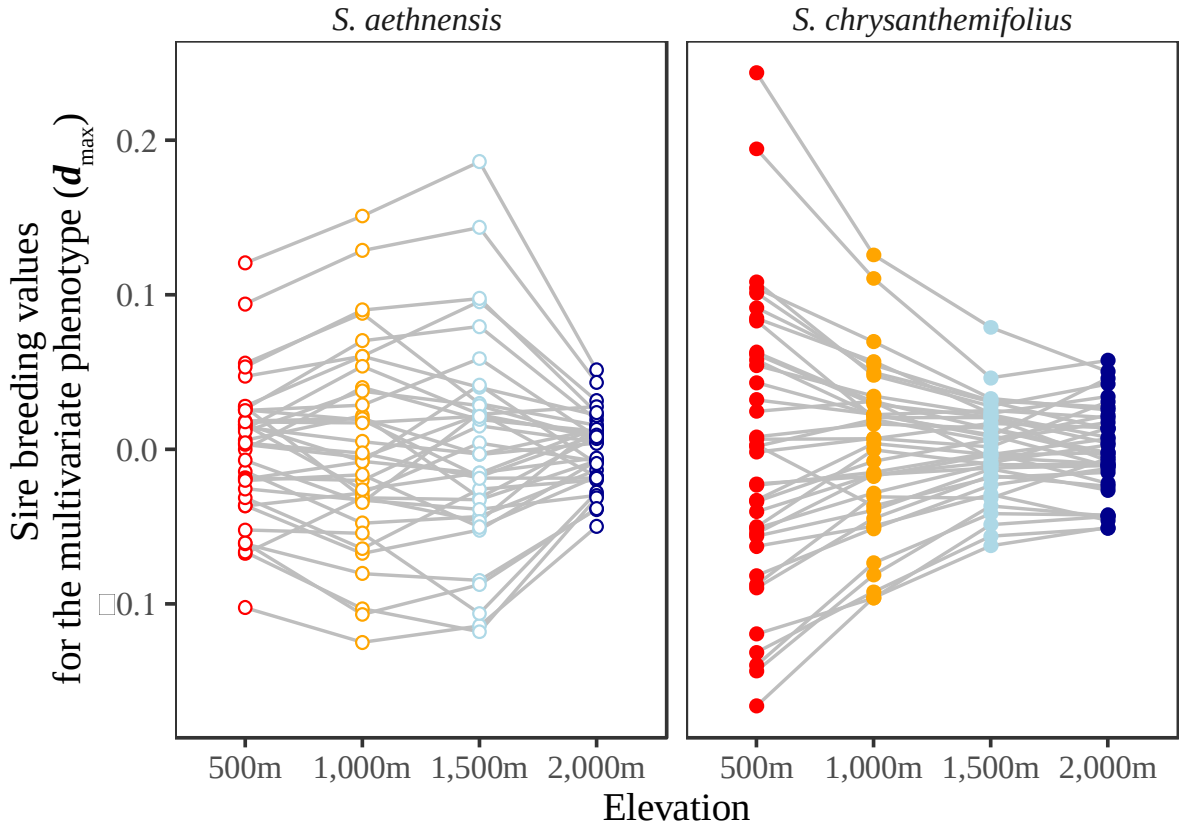

Fig. 6 Sire breeding values for each species at each elevation show how sires change in genetic value relative to each other. Plasticity (as changes in mean phenotype captured by $\boldsymbol{d}_{max}$ from **Fig. 2**) is associated with G×E as a large change in genetic variance across elevation, as well as changes in sire rank across elevation (crossing of sires between elevations).

Discussion

We planted seeds from a breeding design of two closely related but ecologically distinct species across an environmental (elevation) gradient that included each species' native environment and two intermediate environments. We found that estimates of plasticity for eight leaf traits suggested that the phenotype of *S. chrysanthemifolius* moved towards the phenotype of *S. aethnensis* at high elevations, while the phenotype of *S. aethnensis* moved further away from the phenotype of *S. chrysanthemifolius* at lower elevations (**Fig. 2**). This suggests that *S. chrysanthemfolius* shows a more appropriate phenotypic response to a novel environment. Changes in genetic variance across elevation were both significant and stronger than differences between species (**Fig. 3**), and were consistent across elevation for both species (**Fig. 4**). Elevational differences in genetic variance aligned with plasticity as the change in mean phenotype (**Fig. 5**), and were created by patterns of G×E as elevational changes in genetic variance and sire rank (**Fig. 6**). Together, these results suggest that changes in genetic variance occur as a result of G×E underlying phenotypic plasticity in novel environments, which will likely determine the potential for adaptation in novel environments.

By analysing published studies, Wood and Brodie III (2015) found evidence that **G** is likely affected by the environment as much as by evolution, but their results as to why **G** changed in response to the environment were inconclusive. We help to resolve this by showing that novel environments not only create larger changes in **G** than evolutionary history, but that such changes in **G** occur in the direction of plasticity as a consequence of G×E interactions. Our findings not only support an alignment between plasticity and genetic variation (Noble et al. 2019; Johansson et al. 2020), but suggest that to predict evolutionary responses to environmental change, we need to better understand how genetic variation responds to environmental variation. Therefore, future work needs to consider G×E to understand when and how constraints to adaptation will prevent evolutionary rescue in novel environments, and to identify whether environment-dependent genetic constraints could determine evolutionary trajectories.

Our results show that in order to better understand the potential for evolutionary rescue it will be necessary to quantify the prevalence of G×E across a species' range and understand the potential for G×E to maintain ecological resilience in novel environments. Evolutionary rescue will be possible if sufficient G×E in plasticity is available, and selection on genetic variation in plasticity increases fitness in novel environments (Chevin et al. 2010; Chevin and Hoffmann 2017), which can then lead to genetic assimilation of an initially plastic response (Waddington 1953; Lande 2009). Although selection on plasticity should result in rapid adaptation that facilitates evolutionary rescue (Charmantier et al. 2008; Wang and Althoff 2019; Walter et al. 2020), we still do not know whether environmental change will be too extreme or rapid to allow evolutionary

411 rescue. Furthermore, it is likely that in response to novel environments, not only will selection be for the
412 appropriate phenotype (i.e. change in mean phenotype), it is likely that selection for new forms of plasticity
413 that are appropriate to the novel environment (i.e. appropriate fluctuations around the new mean phenotype)
414 will need to evolve. Given the unpredictable nature of novel environments however, selection for a new form
415 of plasticity might be difficult (Leung et al. 2020).

416 The initial resilience of populations exposed to a novel environment will likely depend on how close
417 plasticity is able to move the population towards a phenotypic optimum. Evidence suggests that plasticity in
418 novel environments is more often maladaptive (Langerhans and DeWitt 2002; Palacio-López et al. 2015;
419 Acasuso-Rivero et al. 2019), which means that populations will likely need to rely on rapid adaptation to
420 maintain fitness and prevent extinction. However, there are two major obstacles for evolutionary rescue.
421 Firstly, the adaptive potential for novel environments will be greatly diminished if genetic variance in the
422 direction of selection is low (Walsh and Blows 2009), which can occur if G×E reduces genetic variance in
423 novel environments. We found that the availability of genetic variance for evolutionary rescue will be
424 species-specific. *Senecio aethnensis* showed an increase in genetic variance in the novel environment
425 (500m), which contrasted with *S. chrysanthemifolius*, which showed a decrease in genetic variance at 2,000m
426 (**Table 2**). These results therefore suggest that despite high elevation species having lowered plasticity
427 compared to lower elevation species (Gugger et al. 2015; Schmid et al. 2017; de Villemereuil et al. 2018),
428 selection on increased genetic variation in response to low-elevation (i.e. warmer) conditions could allow
429 evolutionary rescue.

430 Secondly, the potential for rapid adaptation to a novel environment will be determined by the amount of
431 genetic versus phenotypic variance underlying the multivariate phenotype. If plasticity common to all
432 genotypes creates phenotypic variance that hides beneficial genetic variation from selection, then a
433 demographic barrier to adaptation will arise because too few individuals will contribute to the following
434 generation and the populations is more likely to go extinct (Chevin et al. 2013). In other words, if phenotypic
435 variance is biased towards a direction in multivariate phenotype that is different to genetic variance, then it
436 will make adaptation difficult because even if there is substantial genetic variation in the direction of
437 selection, only a small fraction of the population would possess the beneficial alleles and adaptation will be
438 difficult. Comparing genetic and phenotypic variance with the direction of selection using quantitative
439 genetics in reciprocal transplant experiments can therefore identify whether evolutionary rescue in novel
440 environments will be sufficiently rapid to avoid extinction. Such experiments can also be used to predict
441 evolutionary trajectories during adaptation to novel environments by identifying whether evolutionary rescue
442 favours adaptation towards the phenotype of species native to the novel environment, or whether adaptation

favours a different phenotypic optimum.

Although we show that G×E can shift the G-matrix in response to novel environments, whether such shifts can help to promote evolutionary rescue requires estimates of selection and cross-generational selection experiments. A bottleneck event that occurs during the colonisation of (or exposure to) novel environments reduces population size, which can create instability in **G** (Arnold et al. 2008). Evolutionary rescue can only occur in small populations if adaptive alleles increase in frequency rapidly enough to allow adaptation before extinction occurs. Small population sizes can have important consequences for genetic variation by making **G** unstable (Jones et al. 2003). Rapid changes to the orientation and size of **G** can occur when rare alleles held at mutation-selection balance readily increase in frequency (Jones et al. 2003). If such alleles underlie G×E interactions that have low benefit in the native environments, but increase fitness in novel environments (Walter et al. 2020), then the G×E effects of new mutations (Roles et al. 2016) or rare/hidden variants (Schlichting 2008; Brennan et al. 2019) could facilitate evolutionary rescue. It is then likely that mutation will determine whether genetic constraints to rapid adaptation can be overcome for small populations. If pleiotropic mutations that provide beneficial genetic variation in the direction of selection arise readily, then the orientation of **G** can change rapidly for small populations, reducing the constraints to adaptation and making evolutionary rescue more likely (Arnold et al. 2008). Future studies should therefore determine the effect of mutation accumulation on G×E and the response of **G** to novel environments.

Acknowledgements: We are very grateful to Piante Faro (Giarre, Italy) for providing us with glasshouse facilities. We thank Mauro Calvagna for his assistance with the fieldwork, and Giuseppe Riggio for generously providing us access to the 1,000m field site. This work was carried out using the computational facilities of the Advanced Computing Research Centre, University of Bristol. **Funding:** This work was supported by joint NERC grants NE/P001793/1 and NE/P002145/1 awarded to JB and SH. **Data availability:** Upon acceptance, data will be deposited with the Environmental Information Data Centre (UK).

References

Acasuso-Rivero, C., C. J. Murren, C. D. Schlichting, and U. K. Steiner. 2019. Adaptive phenotypic plasticity for life-history and less fitness-related traits. Proceedings of the Royal Society B-Biological Sciences 286.

Aguirre, J. D., E. Hine, K. McGuigan, and M. W. Blows. 2014. Comparing G: multivariate analysis of genetic variation in multiple populations. Heredity 112:21-29.

474 Arnold, S. J. 1992. Constraints on Phenotypic Evolution. The American Naturalist 140:S85-S107.

475 Arnold, S. J., R. Burger, P. A. Hohenlohe, B. C. Ajie, and A. G. Jones. 2008. Understanding the Evolution
476 and Stability of the G-Matrix. Evolution 62:2451-2461.

477 Basser, P. J., and S. Pajevic. 2007. Spectral decomposition of a 4th-order covariance tensor: Applications to
478 diffusion tensor MRI. Signal Processing 87:220-236.

479 Bell, G., and A. Gonzalez. 2009. Evolutionary rescue can prevent extinction following environmental
480 change. Ecology Letters 12:942-948.

481 Brennan, R. S., A. D. Garrett, K. E. Huber, H. Hargarten, and M. H. Pespeni. 2019. Rare genetic variation
482 and balanced polymorphisms are important for survival in global change conditions. Proceedings of
483 the Royal Society B-Biological Sciences 286:20190943.

484 Bylesjo, M., V. Segura, R. Y. Soolanayakanahally, A. M. Rae, J. Trygg, P. Gustafsson, S. Jansson et al.
485 2008. LAMINA: a tool for rapid quantification of leaf size and shape parameters. BMC Plant Biology
486 8.

487 Charmantier, A., R. H. McCleery, L. R. Cole, C. Perrins, L. E. B. Kruuk, and B. C. Sheldon. 2008. Adaptive
488 phenotypic plasticity in response to climate change in a wild bird population. Science 320:800-803.

489 Chenoweth, S. F., H. D. Rundle, and M. W. Blows. 2010. The contribution of selection and genetic
490 constraints to phenotypic divergence. The American Naturalist 175:186-196.

491 Cheverud, J. M. 1984. Quantitative Genetics and Developmental Constraints on Evolution by Selection.
492 Journal of Theoretical Biology 110:155-171.

493 Chevin, L. M., S. Collins, and F. Lefèvre. 2013. Phenotypic plasticity and evolutionary demographic
494 responses to climate change: taking theory out to the field. Functional Ecology 27:966-979.

495 Chevin, L. M., and A. A. Hoffmann. 2017. Evolution of phenotypic plasticity in extreme environments.
496 Philosophical Transactions of the Royal Society of London Series B-Biological Sciences
497 372:20160138.

498 Chevin, L. M., R. Lande, and G. M. Mace. 2010. Adaptation, plasticity, and extinction in a changing
499 environment: towards a predictive theory. PLoS Biology 8:e1000357.

500 de Villemereuil, P., M. Mouterde, O. E. Gaggiotti, and I. Till-Bottraud. 2018. Patterns of phenotypic
501 plasticity and local adaptation in the wide elevation range of the alpine plant *Arabis alpina*. Journal of
502 Ecology 106:1952-1971.

503 Doroszuk, A., M. W. Wojewodzic, G. Gort, and J. E. Kammenga. 2008. Rapid divergence of genetic
504 variance-covariance matrix within a natural population. The American Naturalist 171:291-304.

505 Eroukhmanoff, F., and E. I. Svensson. 2011. Evolution and stability of the G-matrix during the colonization
506 of a novel environment. Journal of Evolutionary Biology 24:1363-1373.

507 Ghalambor, C. K., J. K. McKay, S. P. Carroll, and D. N. Reznick. 2007. Adaptive versus non-adaptive
508 phenotypic plasticity and the potential for contemporary adaptation in new environments. Functional
509 Ecology 21:394-407.

Gomulkiewicz, R., and R. D. Holt. 1995. When does evolution by natural selection prevent extinction? Evolution 49:201-207.

Gugger, S., H. Kesselring, J. Stöcklin, and E. Hamann. 2015. Lower plasticity exhibited by high- versus mid-elevation species in their phenological responses to manipulated temperature and drought. Annals of Botany 116:953-962.

Hadfield, J. D. 2010. MCMC Methods for multi-response generalized linear mixed models: The MCMCglmm R package. Journal of Statistical Software 33:1-22.

Hansen, T. F., and D. Houle. 2008. Measuring and comparing evolvability and constraint in multivariate characters. Journal of Evolutionary Biology 21:1201-1219.

Hine, E., S. F. Chenoweth, H. D. Rundle, and M. W. Blows. 2009. Characterizing the evolution of genetic variance using genetic covariance tensors. Philosophical Transactions of the Royal Society of London Series B-Biological Sciences 364:1567-1578.

Johansson, F., P. C. Watts, S. Sniegula, and D. Berger. 2020. Natural selection mediated by seasonal time constraints increases the alignment between evolvability and developmental plasticity. Evolution.

Jones, A. G., S. J. Arnold, and R. Bürger. 2003. Stability of the G-matrix in a population experiencing pleiotropic mutation, stabilizing selection, and genetic drift. Evolution 57:1747-1760.

Lande, R. 1979. Quantitative genetic analysis of multivariate evolution, applied to brain:body size allometry. Evolution 33:402-416.

—. 1980. The Genetic Covariance between Characters Maintained by Pleiotropic Mutations. Genetics 94:203-215.

—. 2009. Adaptation to an extraordinary environment by evolution of phenotypic plasticity and genetic assimilation. Journal of Evolutionary Biology 22:1435-1446.

Langerhans, R. B., and T. J. DeWitt. 2002. Plasticity constrained: over-generalized induction cues cause maladaptive phenotypes. Evolutionary Ecology Research 4:857-870.

Leung, C., M. Rescan, D. Grulois, and L. M. Chevin. 2020. Reduced phenotypic plasticity evolves in less predictable environments. Ecology Letters 23:1664-1672.

Lynch, M., and B. Walsh. 1998, Genetics and analysis of quantitative traits. Sunderland, Sinauer Associates, Inc.

Martin, G., E. Chapuis, and J. Goudet. 2008. Multivariate Q_{st}–F_{st} Comparisons: A Neutrality Test for the Evolution of the G Matrix in Structured Populations. Genetics 180:2135-2149.

McGlothlin, J. W., M. E. Kobiela, H. V. Wright, D. L. Mahler, J. J. Kolbe, J. B. Losos, and E. D. Brodie, III. 2018. Adaptive radiation along a deeply conserved genetic line of least resistance in *Anolis* lizards. Evolution Letters 2:310-322.

Morrissey, M. B., S. Hangartner, and K. Monro. 2019. A note on simulating null distributions for **G** matrix comparisons. Evolution 73:2512-2517.

Noble, D. W. A., R. Radersma, and T. Uller. 2019. Plastic responses to novel environments are biased

546 towards phenotype dimensions with high additive genetic variation. Proceedings of the National
547 Academy of Sciences, USA 116:13452-13461.

548 Palacio-López, K., B. Beckage, S. Scheiner, and J. Molofsky. 2015. The ubiquity of phenotypic plasticity in
549 plants: a synthesis. Ecology and Evolution 5:3389-3400.

550 R Core Team. 2019 R: A language and environment for statistical computing, version 3.6.1. R Foundation
551 for Statistical Computing, Vienna, Austria.

552 Roles, A. J., M. T. Rutter, I. Dworkin, C. B. Fenster, and J. K. Conner. 2016. Field measurements of
553 genotype by environment interaction for fitness caused by spontaneous mutations in *Arabidopsis*
554 *thaliana*. Evolution 70:1039-1050.

555 Schlichting, C. D. 2008. Hidden reaction norms, cryptic genetic variation, and evolvability. Annals of the
556 New York Academy of Sciences 1133:187–203.

557 Schmid, S. F., J. Stocklin, E. Hamann, and H. Kesselring. 2017. High-elevation plants have reduced
558 plasticity in flowering time in response to warming compared to low-elevation congeners. Basic and
559 Applied Ecology 21:1-12.

560 Via, S., R. Gomulkiewicz, G. De Jong, S. M. Scheiner, C. D. Schlichting, and P. H. Van Tienderen. 1995.
561 Adaptive phenotypic plasticity: consensus and controversy. Trends in Ecology & Evolution 10:212-
562 217.

563 Waddington, C. H. 1953. Genetic Assimilation of an Acquired Character. Evolution 7:118-126.

564 Walsh, B., and M. W. Blows. 2009. Abundant Genetic Variation plus Strong Selection = Multivariate
565 Genetic Constraints: A Geometric View of Adaptation. Annual Review of Ecology, Evolution, and
566 Systematics 40:41-59.

567 Walter, G. M., J. D. Aguirre, M. W. Blows, and D. Ortiz-Barrientos. 2018. Evolution of genetic variance
568 during adaptive radiation. The American Naturalist 191:E108–E128.

569 Walter, G. M., J. Clark, D. Terranova, S. Cozzolino, A. Cristaudo, S. J. Hiscock, and J. R. Bridle. 2020.
570 Hidden genetic variation in plasticity increases the potential to adapt to novel environments. bioRxiv
571 doi: https://doi.org/10.1101/2020.10.26.356451

572 Walter, G. M., S. du Plessis, D. Terranova, E. la Spina, M. G. Majorana, G. Pepe, J. Clark et al. 2021.
573 Adaptive maternal effects in early life history traits help maintain ecological resilience in novel
574 environments for two contrasting *Senecio* species. bioRxiv doi:
575 https://doi.org/10.1101/2021.02.04.429835

576 Wang, S. P., and D. M. Althoff. 2019. Phenotypic plasticity facilitates initial colonization of a novel
577 environment. Evolution 73:303-316.

578 Wood, C. W., and E. D. Brodie III. 2015. Environmental effects on the structure of the G-matrix. Evolution
579 69:2927-2940.

580 Zeng, Z. B. 1988. Long-Term Correlated Response, Interpopulation Covariation, and Interspecific
581 Allometry. Evolution 42:363-374.

582

583

Using a covariance tensor to quantify differences among multiple matrices

Original matrices
4 traits, 4 matrices

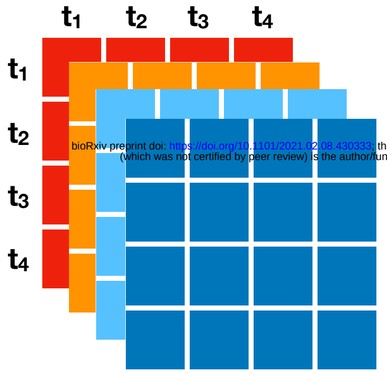

Step 1
Construct the S-matrix, the element-by-element differences among all matrices (i.e. the raw differences)

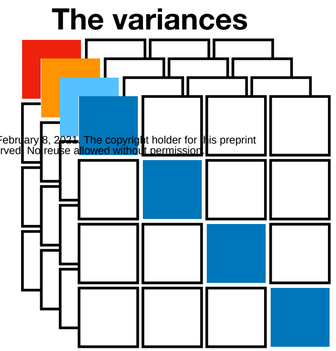

1) Variances of the variances

2) Covariances of the variances

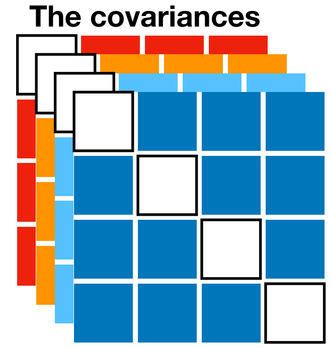

3) Variances of the covariances

4) Covariances of the covariances

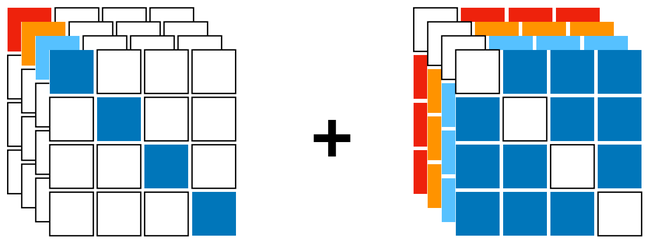

5) Covariances between the variances and covariances

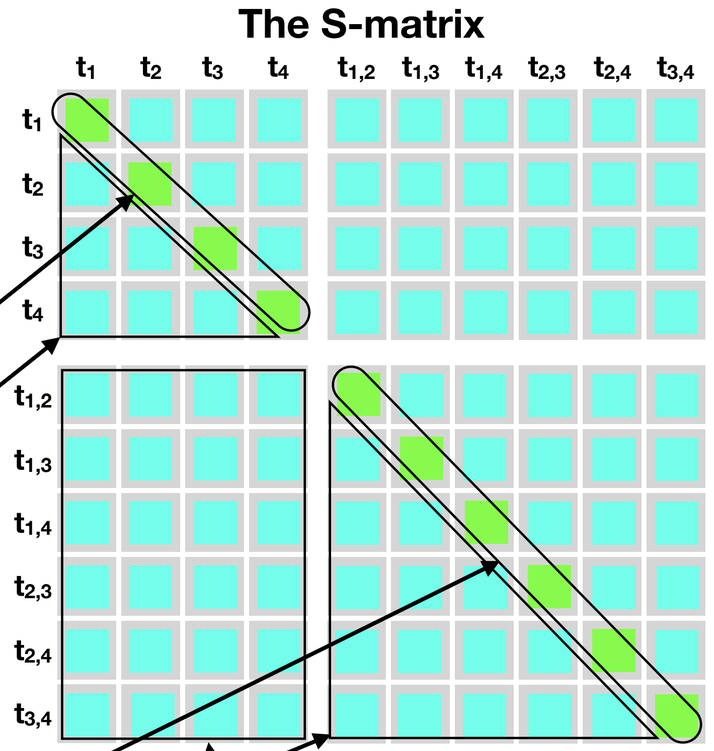

Eigentensors

Constructed from the eigenvectors of **S**

Step 2
Construct eigentensors from the eigenvectors of **S**

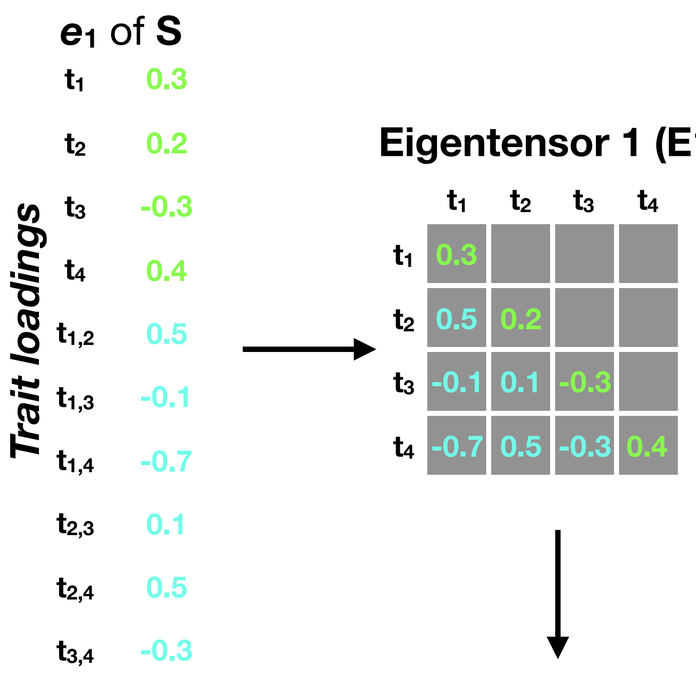

Step 3
Identify how the original traits and matrices contribute to the differences among all matrices described by S

(a) Coordinates - which matrices correlate with the eigentensor

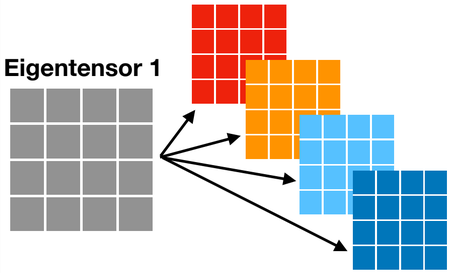

(b) Eigenvectors of eigentensors - how do the original traits contribute to the eigentensors